Contents lists available at ScienceDirect

Journal of Electrostatics

journal homepage: http://www.elsevier.com/locate/elstat

Reduction of dust emission by Coromax micro-pulse power supplies at an oil shale fired power plant

B. Bidoggia *, M.K. Larsen, K. Poulsen, K. Skriver

FLSmidth Airtech, Vigerslev allé 77, 2500, Valby, Denmark

ARTICLE INFO

Keywords:
Electrostatic precipitator
Power supplies
Micro-pulse energization
T/R sets
SMPS

ABSTRACT

Several classes of power supplies for ESP exist and the choice of the correct class is related to the resistivity of the dust to filter. The case of a power plant with high-resistivity dust emissions, for which the replacement of the existing power supplies with micro-pulse power supplies has succeeded in halving the dust emission level, is presented. The presentation is completed with data measured before and after the installation of the new power supplies and with a simplified analytical explanation supporting the results.

1. Introduction

This paper deals with the case of the oil-shale fired power plant, Balti Power Plant (hereinafter the Plant) near Narva in Estonia, owned by Eesti Energia.

Estonia massively uses oil shale, an organic-rich fine-grained sedimentary rock with a caloric heating value lower than hard coal and with higher ash content than lignite, for electricity production. The oil shale is burned in traditional boilers and the fumes are dedusted by electrostatic precipitators (ESPs) [1].

The three main typical voltage waveforms used in energization of ESPs are constant or almost constant voltage, voltage with grid-frequency ripple and voltage with microsecond-range pulses (Fig. 1).

These voltage waveforms need to be adapted to the resistivity of the dust to be filtered: typically, a constant or almost constant waveform is used for low-resistivity dust ($\rho < 1{\cdot}10^{-7}$ Ωm), a grid-frequency ripple waveform is used for medium-resistivity dust ($1{\cdot}10^{-7}$ Ωm $< \rho < 5{\cdot}10^{-9}$ Ωm) and a micro-pulse waveform is used for medium and high-resistivity dust ($\rho > 5{\cdot}10^{-9}$ Ωm) [2,3].

Different classes of power supplies are used to create the required voltage waveforms as summarized in Table 1 [4].

Transformer/rectifier (T/R) sets, switch mode power supplies (SMPS)—often referred to as high-frequency power supplies—and voltage source converter (VSC)—often referred to as medium-frequency power supplies—can technically all provide the two waveforms adapted for low and medium resistivity.

Because of the large electrical time constant typical for an ESP—in the order of several milliseconds—, microsecond-range pulses can only be created by a special class of power supplies, here referred to as micro-pulse power supplies (MPPS). These are special power supplies, composed of two independent power supplies coupled by a resonant circuit [4,5].

In some cases of medium-high resistivity dust and under some limitations, it might still be possible to use single-phase T/R sets or SMPSs using the intermittent energization (IE) control technique [5].

At the Plant, substituting three SMPSs with three MPPSs succeeded in achieving the required low emission level, which otherwise could not be reached because of the high resistivity of the ashes.

In the Materials and Methods section, the description of the ESP in the Plant before and after the installation of the MPPSs is presented. It is completed by measurements of the original operation of the ESP. The section also includes the mathematical analysis used in the calculation of the power consumption and in the comparison of the ESP efficiency for the different classes of power supplies.

The Results section contains the measurements of voltage levels and power consumption obtained after the installation of the MPPSs, and the comparison with the original values. It also contains the measurements of dust emission levels and the comparison with the original values. The total mass efficiency of one section of the ESP for the different classes of power supplies for one specific case is also traced.

The Discussion and Conclusion sections follow, where the results are commented.

* Corresponding author.
E-mail address: bebi@flsmidth.com (B. Bidoggia).

https://doi.org/10.1016/j.elstat.2020.103447
Received 2 July 2019; Received in revised form 2 January 2020; Accepted 2 March 2020

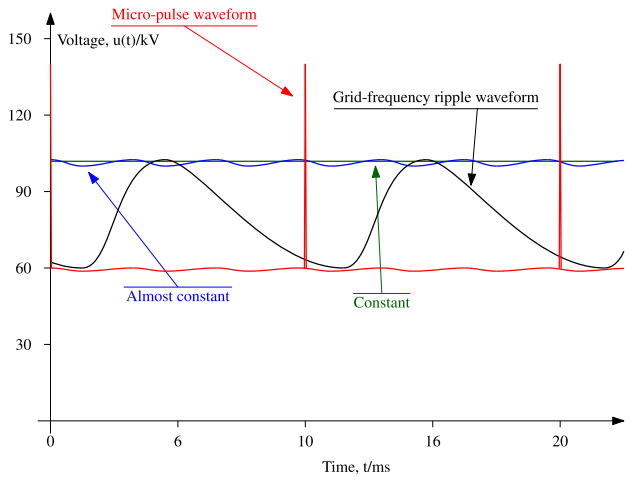

Fig. 1. Comparison of the main typical waveforms used in energization of ESPs.

Table 1
Comparison of classes of power supplies: T/R set (T/R), switch-mode power supplies (SMPS), voltage-source converters (VSC), micro-pulse power supplies (MPPS).

Class	Waveforms	
	Constant	Ripple
T/R	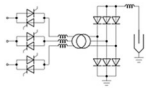	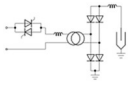
SMPS	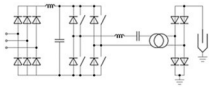	
VSC	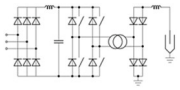	
	Micropulse	
MPPS	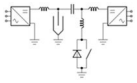	

2. Materials and methods

This section is divided into four parts. The first part describes the setup of the plant and of the ESP under consideration, with its history. The second part is an analytical derivation of the equations linking ESP power and ESP mean voltage in the most generic case for SMPSs and MPPSs. The third part is an analytical derivation of the equations linking ESP filtration efficiency and ESP mean and peak voltages in the most generic case for SMPSs and MPPSs. The fourth part is an analytical derivation of the constraints linking ESP mean and peak voltage values in the most generic case for SMPSs and MPPSs.

Setup of the plant and ESP history — The Plant consists of two blocks, called block 8 and block 11. The nominal power of each block is equal to 215 MW, and each of them consists of 2 boilers with individual precipitators (Fig. 2).

The four ESPs were built by Alstom in 2004, and each consists of 1 chamber with 4 fields, with 1 section per field. The total collection area per ESP is about 16 000 m^2; the capacitance of each section is 84 nF.

This paper focuses on the ESP 8K-2, whose nominal mass flow on a wet basis is 432 000 Nm^3/h at 190 °C with a water content of 13% in volume. The dust concentration at the inlet was equal to 120 g/Nm^3 on a wet basis and the dust resistivity was measured equal to $1 \cdot 10^9$ Ωm.

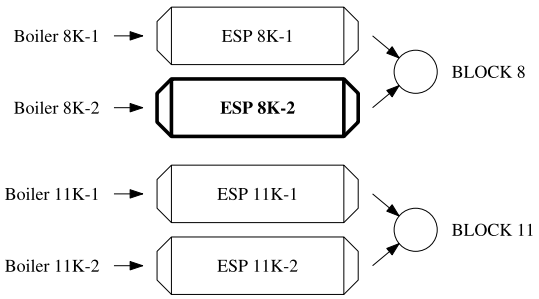

Fig. 2. Blocks, boilers, and ESPs of the Plant.

The ESP was originally designed to guarantee a maximum emission level of 50 mg/Nm^3 and with the introduction of new regulations, the system needed to be retrofitted to lower the emission level to 20 mg/Nm^3. It was originally powered by single-phase T/R sets.

A first attempt to reduce the emission level included minor mechanical repairs and the substitution of the original T/R sets with SMPSs from a first manufacturer. Since the emission levels were still above the desired level, two other different types of SMPSs from a second and a third manufacturer were installed. The final configuration is shown in Fig. 3, with emission levels still above the required limit.

It is reasonable to assume that, after each installation of the three different types of SMPSs, all the necessary mechanical modifications and optimization of the rapping timers had been performed to try to achieve the required emission levels.

During an inspection in July 2016, the operating values for the four sections of ESP 8K-2 were recorded (Table 2).

In March 2017, three MPPSs were ordered and then installed on sections 2, 3 and 4 of ESP 8K-2 in replacement of the existing SMPSs. The MPPSs are FLSmidth Coromax 4: their nominal base voltage is 60 kV, their nominal pulse voltage is 80 kV, their nominal output current is 1000 mA, their nominal pulse width is 75 μs, and their maximum pulse repetition frequency is 100 Hz; they are powered by the 400 V three-phase low-voltage grid. The MPPSs were commissioned in June 2017.

The new configuration of the power supplies of the ESP is presented in Fig. 4. An aerial view of the roof of the ESP with the new power supplies is presented in Fig. 5 and a close view of one of the MPPSs after installation is presented in Fig. 6.

Minor mechanical modifications were also performed, like the installation of new baffle plates. The commissioning procedure also included the optimization of the rapping timing for all the sections of the ESP.

Analytical derivation of ESP power — To compare and analytically explain the power consumption before and after the installation of the MPPSs, the following assumptions were made.

For an SMPS, because of the very small ripple, the secondary voltage and current can be assumed constant as

$$u_{dc}(t) \equiv U_{dc} \tag{1}$$

$$i_{dc}(t) \equiv I_{dc} \tag{2}$$

and the secondary power can therefore be calculated as

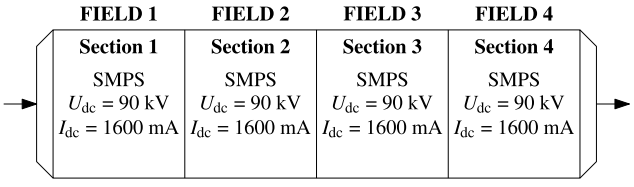

Fig. 3. Configuration of the power supplies of the ESP before the installation of the MPPSs. U_{dc} and I_{dc} represent the nominal secondary dc voltage and current.

Table 2
Measured mean secondary voltage (U_{dc}), peak secondary voltage (U_t), mean secondary current (I_{dc}), spark frequency (f_{sp}) for the four sections (F) of ESP 8K-2 before the installation of the MPPSs. T indicates the type of power supply: S for SMPS.

F	T	U_{dc}/kV	U_t/kV	I_{dc}/mA	f_{sp}/(1/min)
1	S	70	70	1560	13
2	S	70	70	1570	0
3	S	55	55	1550	0
4	S	59	59	1550	0

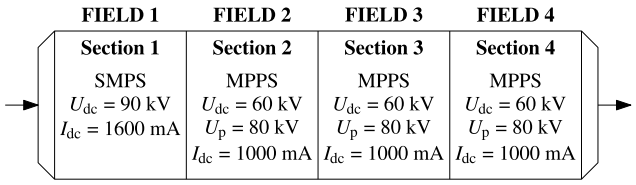

Fig. 4. Configuration of the power supplies of the ESP after the installation of the MPPS. U_{dc}, U_p and I_{dc} represent the nominal secondary dc voltage, pulse voltage, and current.

$$P_{dc} = U_{dc}\ I_{dc}\ . \tag{3}$$

For an MPPS, the pulsing components need to be considered and the secondary voltage and current can be expressed as

$$u_{dc}(t) = U_{dc} + u_p(t) \tag{4}$$

$$i_{dc}(t) = I_{dc} + i_p(t); \tag{5}$$

However, the pulsing voltage and current are mainly related to reactive power and the secondary power can be calculated as

$$P_{dc} \cong U_{dc}\ I_{dc}\ + cU_pI_{dc}, \tag{6}$$

where the value of the constant c has been found experimentally and is reported in the literature ($c \cong 0.5$) [5].

Analytical derivation of ESP efficiency — To compare and analytically explain the difference in the efficiency of an ESP between single-phase T/R sets (1-T/Rs), three-phase T/R sets (3-T/Rs), SMPSs and MPPSs, the total mass efficiency of a section (η) has been related to the values of peak (U_t) and mean (U_{dc}) voltage of the section itself, to which correspond the values of peak (E_t) and mean (E_{dc}) electric field.

The maximum obtainable charge (q) for a particle is proportional to the peak value of the electric field (E_t) and can be expressed by Ref. [6].

$$q = k_qE_t, \tag{7}$$

where k_q depends on the particular geometry.

The electrical force (F) acting on a dust particle in the direction of the collecting plates is proportional to the mean value of the electric field (E_{dc}) and of the particle charge, and it can be expressed as [6].

$$F = qE_{dc} = k_qE_tE_{dc}. \tag{8}$$

The migration velocity (w) of a particle in the electric field is proportional to the force acting on it as expressed by Stokes' law [6].

$$w = k_wF = k_wk_qE_tE_{dc}, \tag{9}$$

where k_w depends on the particular geometry and on the property of the fluid in which the particle is moving.

The total mass efficiency of a section can be expressed by the Deutsch equation [5].

$$\eta = 1 - e^{-\frac{wA}{Q}}, \tag{10}$$

where A is the cross-sectional area and Q is the mass flow of the gas, and by substituting (9) in (10)

$$\eta = 1 - e^{-\frac{k_wk_qE_tE_{dc}A}{Q}}. \tag{11}$$

The electric field (E) inside a section is directly proportional to the voltage applied to it (U) as

$$E = k_EU, \tag{12}$$

where k_E depends on the particular geometry.

The total mass efficiency of a section can thus be rewritten as

$$\eta = 1 - e^{-\frac{k_wk_qk_E^2U_tU_{dc}A}{Q}} = 1 - e^{-k_\eta U_tU_{dc}} \tag{13}$$

Showing that the higher the peak (U_t) and mean (U_{dc}) voltages, the higher the efficiency is.

Constraints on ESP peak voltage — The peak voltage (U_t) is limited by the breakdown voltage (U^*) of the gas inside the section

$$U_t \le U^*. \tag{14}$$

For 1-T/Rs, 3-T/Rs and SMPSs, this also limits the mean voltage (U_{dc}) since

$$U_t = \xi U_{dc} \tag{15}$$

where $\xi \cong 1.2$ for the former class, while $\xi = 1$ for the latter two classes.

For MPPSs, the voltage is the sum of a base voltage (U_b) and of a pulse voltage (U_p), which can be independently adjusted. The peak voltage (U_t) is the sum of base and pulse voltages and is limited by the breakdown voltage of the gas inside the section

$$U_t = U_b + U_t \le U_p^*. \tag{16}$$

Also, because of the mechanisms of discharge in presence of micro-

Fig. 5. Aerial view of the roof of the ESP.

Fig. 6. Close view of one of the MPPSs after installation.

Table 3
Mean voltage (U_{dc}), pulse voltage (U_p), peak voltage (U_t), mean current (I_{dc}), spark frequency (f_{sp}) for the four sections (F) of ESP 8K-2 after the installation of the MPPSs in September 2017. T indicates the type of power supply: S for SMPS, P for MPPS.

F	T	U_{dc}/kV	U_p/kV	U_t/kV	I_{dc}/mA	f_{sp}/(1/min)
1	S	72	n/a	72	1500	> 0
2	P	50	50	100	800	13
3	P	46	60	106	800	11
4	P	43	65	108	800	2

Table 4
Comparison of peak voltage before ($U_{t,1}$) and after ($U_{t,2}$) the installation of the MPPSs for the four sections (F) of ESP 8K-2. k_u is the ratio $U_{t,2}/\ U_{t,1}$. T indicates the type of power supply: S for SMPS, P for MPPS.

F	Before		After		k_u
	T	$U_{t,1}$/kV	T	$U_{t,2}$/kV	
1	S	70	S	72	1.0
2	S	70	P	100	1.4
3	S	55	P	106	1.9
4	S	59	P	108	1.8

pulses is different, the breakdown voltage (U_p^*) for the gas inside the sections powered by MPPSs is typically higher than the breakdown voltage (U^*) for the gas inside the sections powered by 1-T/Rs, 3-T/Rs or SMPSs, and can be expressed by

$$U_p^* = \gamma U^* \tag{17}$$

with $\gamma > 1$.

Because of the narrow pulses, the contribution of U_p to the mean voltage is negligible. Therefore, the base voltage and the mean voltage can be confused

$$U_{dc} \cong U_b. \tag{18}$$

Although the pulse of voltage is typically shorter than 100 μs, the duration of the related electric field is in the order of several milliseconds, which is longer than the time required to charge to saturation the particles. This ensures the validity of (13) for all types of power supplies, including MPPSs [5].

3. Results

This section is divided into two parts. The first part describes the operation of the ESP after the installation of the MPPSs. The second part presents the plots of the analytical functions of peak voltage and filtration efficiency versus mean voltage for a generic case, where the values of the constants introduced in the previous sections have been chosen to highlight the differences between the power supplies.

Operation of the ESP with MPPS — The operating electrical values for all the power supplies of 8K-2 measured after optimizing the parameters of the MPPSs are reported in Table 3. The peak voltage, which corresponds to the maximum voltage attainable, for the sections powered by an MPPS is between 39% and 50% higher than for the first section, which is powered by an SMPS.

The measurements of peak secondary voltage were also compared section by section for the two conditions before and after the installation of the MPPSs, and are reported in Table 4. The peak secondary voltages were between 40% and 90% higher for the sections supplied by an MPPS, while it was the same for the first section.

The secondary power before and after the installation of the MPPSs was derived from the operation values and reported in Table 5. The secondary power decreased to between 36% and 43% of the original value for the sections supplied by an MPPS, while it was the same for the first section.

Table 5
Comparison of power before ($P_{dc,1}$) and after ($P_{dc,2}$) the installation of the MPPSs for the four sections (F) of ESP 8K-2. k_p is the ratio $P_{dc,2}/P_{dc,1}$. T indicates the type of power supply: S for SMPS, P for MPPS.

F	Before		After		k_p
	T	$P_{dc,1}$/kW	T	$P_{dc,2}$/kW	
1	S	109	S	108	0.99
2	S	110	P	60	0.55
3	S	85	P	61	0.71
4	S	91	P	60	0.66

Table 6
Dust concentration measured in August 2017 after the installation of the MPPSs; δ_A indicates the raw measurements, while δ_B indicates the measurements corrected to 6% of O_2; the measurements intervals are in accordance with the EN 13284 standards "Stationary source emissions—Determination of low range mass concentration of dust," which is used for performance tests.

Interval	δ_A/(mg/m^3)	δ_B/(mg/m^3)
11:00–12:00	7	12
13:00–14:00	8	14
14:00–15:00	7	12
Average	7.3	12.7

The dust concentration after ESP 8K-2 was measured and is reported in Table 6. The average dust concentration corrected to 6% of O_2 is 64% of the guaranteed value (20 mg/Nm^3).

The dust concentration levels for 8K-1 and for 8K-2 after the installation of the MPPSs were also measured for two different operating conditions of the boiler and is reported in Table 7. The ratio of the dust concentration after the two ESPs was calculated. On average the ESP powered by MPPSs presents around half of the dust concentration of the ESP powered by SMPSs.

Analytical functions of filtration efficiency and peak voltage — To illustrate the effect of the increased peak voltage on the ESP efficiency, the case of section 3 has been taken as an example.

The peak voltage (U_t) for the different classes of power supplies has been plotted as an analytical function of the mean voltage (U_{dc}) in Fig. 7.

The effect of the mean voltage, peak voltage, and breakdown voltage is shown in Fig. 8 as the analytical function of the efficiency of the section versus mean voltage, where the constant k_η of (13) has been arbitrarily chosen to highlight the differences between the classes of power supplies.

4. Discussions

The peak secondary voltage for the sections with MPPSs was much higher than the peak secondary voltage for the section with SMPS, and for the same sections before the installation of the MPPSs for the same operating conditions. The same peak secondary voltage on the first section, where the SMPS had not been changed, is an indicator of having

Table 7
Comparison of measured dust concentrations δ_o between ESP 8K-1 (without MPPSs) and ESP 8K-2 (with MPPSs); k_δ is the ratio in dust concentration with and without MPPSs (measurements corrected to 6% of O_2); the measurements consist of two sets of measurements, each one 1-h long, performed during two different days (4 January 2018 and 5 January 2018, by the operator of the plant).

Condition	δ_o/(mg/Nm^3)		k_δ
	8K-1 (w/o MPPS)	8K-2 (w/ MPPS)	
(a)	26	17	0.65
(b)	35	16	0.46
Average	30.5	16.5	0.54

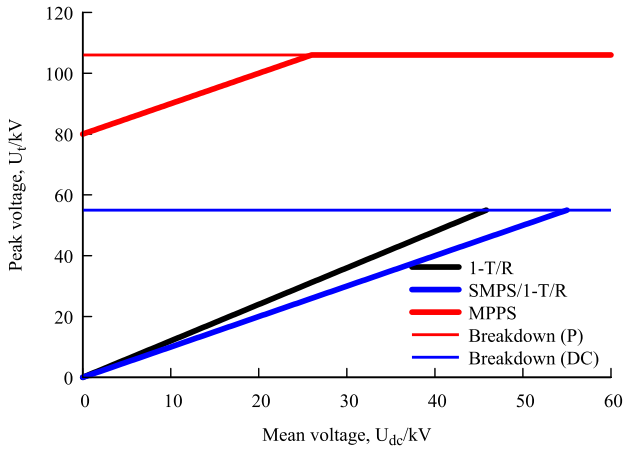

Fig. 7. Peak voltage as an analytical function of the mean voltage for the different classes of power supplies.

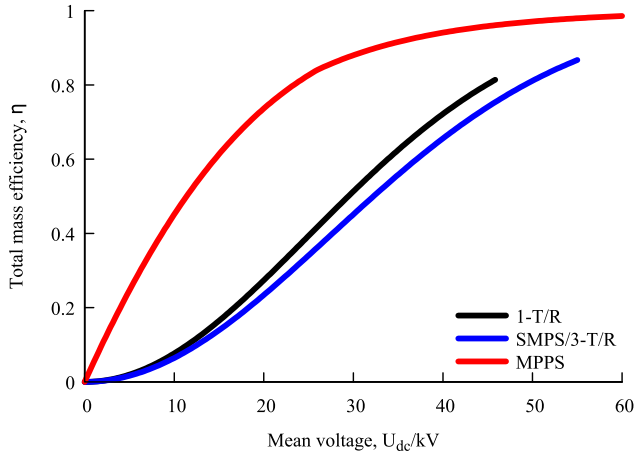

Fig. 8. Analytical function of the efficiency of a section versus mean voltage where the constant of the exponential function has been arbitrarily chosen to highlight the differences between the classes of power supplies.

compared the ESP under similar operating conditions.

In general, under the same operating conditions, and, therefore, under the same electrical conditions of the gas, the breakdown voltage of the gas inside a section powered by a 1-T/R set, a 3-T/R set or by an SMPS is the same. Since the breakdown voltage limits the peak voltage, SMPSs and 3-T/R sets can equally provide a higher average voltage than 1-T/R sets, which yields to a higher filtering efficiency of the ESP.

On the other side, MPPSs can generate pulses which are narrow enough to influence the mechanism of discharge and can, therefore, increase the breakdown voltage of the gas. As a result, the achievable peak voltage is even higher, which yields to an even higher filtering efficiency of the ESP.

Because the higher peak voltage of an MPPS does not necessarily entail a higher mean voltage and, therefore, a higher mean current, an MPPS requires less power for achieving the same or higher filtering efficiency compared to the other classes of power supplies [7].

Because of the higher peak voltage, an ESP powered by MPPSs has a higher total mass efficiency compared to the other classes of power supplies. This is particularly evident for medium- and high-resistivity dust, for which the back-corona phenomenon is one of the main limitations for the other classes of power supplies [8].

This comparison between SMPSs and MPPSs does not consider factors like complexity and purchase price of the power supplies themselves. These factors, which depend on the particular manufacturers, enter into play in the financial analysis of the different solutions available and able to deliver the expected results. They are therefore beyond the scope of this paper.

5. Conclusion

This paper dealt with the case of an oil-shale fired power plant, for which changing the power supplies of an ESP from switch-mode power supplies (SMPSs) to micro-pulse power supplies (MPPSs) has halved the dust emission level. At the same time, this has also yielded a reduction in power consumption. The configuration of the ESP together with the operational data before and after the installation of the MPPSs has been presented. A simplified analytical explanation of why MPPSs have higher filtering efficiency than other classes of power supplies was also given.

The installation of three MPPSs instead of existing SMPSs has succeeded in reducing the emission levels caused by high-resistivity dust to the levels required by the law. This solution was cheaper and required a shorter downtime than other solutions, like the extension of the ESP or the conversion to a fabric filter.

The type of the installed MPPSs was FLSmidth Coromax 4, which is the reference in the market for what concerns MPPSs because of its long tradition, its maturity level, and its proven performance.

Declaration of competing interest

The authors declare that they have no known competing financial interests or personal relationships that could have appeared to influence the work reported in this paper.

Acknowledgments

Thanks are due to Jevgeni Ossovik and Jelena Derbneva of Eesti Energia AS for providing useful information and comments.

References

[1] J.R. Dyni, Geology and resources of some world oil-shale deposits: U.S, Geol. Surv. Sci. Invest. Rep. (2006) 15–17, 2005–5294.
[2] H.J. White, Industrial Electrostatic Precipitation, International Society for Electrostatic Precipitation, 1963.
[3] V. Reyes, K. Poulsen, Use of three-phase rectifiers in ESP's for low resistivity applications, in: Proc. 13th Int. Conf. On ESP (ICESP), Bangalore, India, 16–21 September, 2013.
[4] N. Grass, W. Hartmann, M. Klockner, Application of Different Types of High-Voltage Supplies on Industrial Electrostatic Precipitators, IEEE Transactions on Industry Applications, 2004, pp. 1513–1520.
[5] K.R. Parker, Applied Electrostatic Precipitation, Blackie academic and professional, 1997.
[6] F.L. Smidth, Electrostatic Precipitators Handbook, 1984.
[7] N. Yamamura, O. Tanaka, K. Takahashi, Operating experience of a pulse ESP at a modern 500 MW coal fired power plant in Japan, in: Proc. 6th Int. Conf. On ESP (ICESP), Budapest, Hungary, 18–21 June, 1996.
[8] S. Masuda, Resistivity and back corona, in: Proc. Int. Conf. On Electrostatic Precipitation, Montrey, CA. U.S.A., 14–16 October, 1981.